

A variable 0.58–2.44 Hz quasi-periodic oscillation in the eclipsing and dipping low-mass X-ray binary EXO 0748–676

Jeroen Homan¹, Peter G. Jonker¹, Rudy Wijnands¹, Michiel van der Klis¹, Jan van Paradijs^{1,2}

ABSTRACT

We report the discovery of a quasi-periodic oscillation (QPO) in data obtained with the Rossi X-ray Timing Explorer of the dipping and eclipsing low-mass X-ray binary EXO 0748–676. The QPO had a frequency between 0.58 and 2.44 Hz changing on time scales of a few days, an rms amplitude between 8% and 12%, and was detected in the persistent emission, during dips and during type I X-ray bursts. During one observation, when the count rate was a factor 2 to 3 higher than otherwise, the QPO was not detected. The strength of the QPO did not significantly depend on photon energy, and is consistent with being the same in the persistent emission, both during and outside the dips, and during type I X-ray bursts. Frequency shifts were observed during three of the four X-ray bursts. We argue that the QPO is produced by the same mechanism as the QPO recently found by Jonker et al. (1999) in 4U 1323–62. Although the exact mechanism is not clear, it is most likely related to the high inclination of both systems. An orbiting structure in the accretion disc that modulates the radiation from the central source seems the most promising mechanism.

Subject headings: accretion, accretion disks - stars: individual (EXO 0748–676) - stars: neutron - X-rays: stars

¹Astronomical Institute 'Anton Pannekoek', University of Amsterdam, and Center for High Energy Astrophysics, Kruislaan 403, 1098 SJ, Amsterdam, The Netherlands

²University of Alabama in Huntsville, Department of Physics, Huntsville, AL 45899

1. Introduction

The low-mass X-ray binary (LMXB) EXO 0748–676 was discovered with *EXOSAT* by Parmar et al. (1985). It showed periodic eclipses, irregular intensity dips, and type I X-ray bursts (Parmar et al. 1986). The eclipses, due to obscuration of the central X-ray source by the companion star, occurred at a period of 3.82 hr. From the eclipse duration an inclination of 75° to 82° was derived. Dipping activity is seen at orbital phases $\phi \sim 0.8 - 0.2$ and at $\phi \approx 0.65$ ($\phi = 0$ corresponds to eclipse center). The dips can be as deep as 100% (Church et al. 1998). It is believed (White & Swank 1982; Walter et al. 1982) that such dips are caused by obscuration of the central X-ray source by a bulge in the outer accretion disk that is created by the impact of the gas stream from the companion star, or by the accretion stream itself if it penetrates the disk further in (Frank, King, & Lasota 1987). During the eclipses 4% of the 2–6 keV intensity remained, which Parmar et al. (1986) attributed to the presence of an accretion disk corona (ADC). Using their ‘progressive covering’ model Church et al. (1998) found that $\sim 70\%$ of the out-of-dip flux is contributed by this ADC, which they estimated to have a radius of $0.4\text{--}1.5 \times 10^8$ cm.

Recently, a persistent 1 Hz quasi-periodic oscillation (QPO) was found with RXTE in the high inclination ($i \approx 80^\circ$) dipping LMXB 4U 1323–62 (Jonker, Van der Klis, & Wijnands 1999, hereafter JO99). JO99 concluded that its presence is most likely related to the high inclination of the system. In this Letter, we report the discovery of a variable 0.58–2.44 Hz QPO in EXO 0748–676 with properties similar to those found in 4U 1323–62.

2. Observation and Analysis

We made use of data obtained with the proportional counter array (PCA; Jahoda et al. 1996) on board the *Rossi X-ray Timing Explorer* (*RXTE*; Bradt, Rothschild, & Swank 1993). A

log of all observations is given in Table 1. Observations 2 to 7 were originally performed to study the orbital evolution of the system. Each consisted of five ~ 2 ks data intervals that range in orbital phase from $\phi \approx 0.9$ to $\phi \approx 0.05$. All observations yielded data in the Standard 1 and 2 modes, which have 1/8 s time resolution in 1 energy channel (2–60 keV) and 16 s time resolution in 129 channels (2–60 keV), respectively. In addition, data were obtained in modes with at least 2^{-12} s time resolution, in 67 (obs. 1), 32 (obs. 2), 256 (obs. 2–7), or 64 (obs. 8–10) channels, covering the 2–60 keV range. Data during eclipses were removed from further analysis. X-ray bursts were studied separately.

Power spectra were created in the energy bands 2–60, 2–5, 5–8, 8–13, and 13–42 keV. The average 1/16–128 Hz power spectra of each observation were rms normalized, and fitted with a model consisting of a constant (representing the Poisson level), a power law, $P \propto \nu^{-\alpha}$ (the noise component), and a Lorentzian (the QPO). Errors on the parameters were determined using $\Delta\chi^2 = 1$. The dependence on photon energy of the QPO strength was determined by fitting the power spectra in four energy bands, while keeping the QPO FWHM and frequency, and the power law index (α) of the noise component fixed to the values obtained in the 2–60 keV band. Unless stated otherwise the fit parameters are those in the 2–60 keV band. The 95% confidence upper limits on the presence of the QPO and/or noise component were determined by fixing the FWHM and frequency, and/or by fixing α .

For observations 2–6 and 8–10 we compared power spectra obtained in- and outside the dips. A count rate level was determined for each single orbit, below which data were assumed to be in a dip. For observations 8–10 this level was the persistent count rate during phases where normally no dipping is observed. As mentioned before, observations 2–6 were taken during phases that normally show dipping, which is confirmed by increases in hardness. For these observations we

took the post-eclipse count rate as the discriminator, since dipping usually occurs less after the eclipse.

3. Results

Figure 1 shows two typical power spectra of EXO 0748–676. A QPO peak was found in the power spectra of all observations except the first one. The QPO covered a frequency range of more than a factor 4, between 0.58 ± 0.01 Hz (obs. 10) and 2.44 ± 0.03 Hz (obs. 2), with rms amplitudes between $8.4\% \pm 0.4\%$ and $12.1\% \pm 0.6\%$. Within each observation (~ 1 day) the QPO was only observed in a small frequency range, never changing more than 15% in frequency. Table 1 gives the fit parameters of all observations in the 2–60 keV energy band. In observation 1, where the QPO was not detected, i.e., at least a factor 4 weaker than otherwise, the background corrected count rate was a factor 2 to 3 higher than in the other observations. In the other observations, neither the QPO nor the noise component show any correlation between their parameters and the 2–60 keV count rate, which varies by $\sim 20\%$. However observations 8, 9, and 10, for which (due to the more extended phase coverage) the persistent count rate could be estimated much better than for the other observations, show a clear anti-correlation between frequency and count rate. The QPO peak becomes broader when its frequency increases (see Figure 2). The ratio Q , of frequency over FWHM of the QPO, is consistent with being constant; a linear fit gives a Q of 3.5 ± 0.1 , with $\chi^2/\text{d.o.f.} = 12.2/8$. The noise component tends to become steeper as it gets stronger (see Figure 3). The rms of the QPO decreases from $\sim 12\%$ to $\sim 8.5\%$ when the rms of the noise component increases from $\sim 6\%$ to $\sim 10.5\%$. Although there is considerable scatter around a linear relation, there seems to be a connection between the two components (correlation coefficient is -0.75). Figure 4 shows the photon energy spectra of the QPO in observations 2 to 10 (dip and non-dip data combined). It is obvious from

this figure that they are quite flat. The energy spectra of the noise component are similar.

All QPO parameters in- and outside the dips are consistent with each other, except for the QPO amplitude in observation 10, which during the dips is $12.0\% \pm 0.8\%$ rms and outside the dips $7.5\% \pm 0.4\%$ rms. The noise shows only a significant difference in observation 4, where the dip rms is $9.6 \pm 0.5\%$ and the non-dip rms is $14.9 \pm 1.4\%$.

Four type I X-ray bursts were observed, all outside dips; one in observations 5 and 8 each, and two in observation 9 (hereafter burst 1 to 4). In 16 s resolution data they had peak count rates (2–60 keV, 3 detectors, background corrected) of 2330 ± 10 , 2240 ± 10 , 2410 ± 10 , and 2110 ± 10 counts s^{-1} , respectively, and they all lasted ~ 400 s. In all four bursts the QPO was detected. The QPO during burst 2 is the only that has width and frequency that are consistent with those of the QPO outside the burst. The QPO frequency during burst 1 is 0.1 Hz higher than that of the QPO outside the burst, and the FWHM is 0.18 ± 0.05 Hz, which is considerably smaller than 0.36 Hz. The QPOs during bursts 3 and 4 are both poorly fitted with a Lorentzian. Both peaks appear to have shifted in frequency during the bursts. The peaked shape in the power spectrum of burst 4 clearly consists of two small peaks, which, when fitted with Lorentzians, have frequencies of 0.65 ± 0.05 Hz and 0.89 ± 0.02 Hz and a FWHM of ~ 0.1 Hz. The QPO in burst 3 is very asymmetric. The best fit with one Lorentzian at 0.74 ± 0.02 Hz and a FWHM of ~ 0.1 Hz, shows excess power at higher frequencies. Dynamical power spectra of burst 3 and 4 show that the QPO profile changed with time. The QPOs during the four bursts have rms amplitudes of $9.7\% \pm 0.9\%$, $8.4\%_{-1.0}^{+1.2\%}$, at least 7% (probably 8%–10%), and $\sim 10\%$ (the sum of the rms amplitudes of the two Lorentzians), respectively, consistent with those found outside the bursts.

4. Discussion

We have discovered a QPO in EXO 0748–676 with a frequency varying between 0.58 and 2.44 Hz, and with rms amplitudes between 8.4% and 12.1%. The QPO was detected throughout the persistent emission, the dips, and the type I X-ray bursts, with strengths that were consistent with each other, except in observation 10, where the QPO was stronger during the dips than in the persistent emission. Over the whole frequency range Q was consistent with 3.5, except in the X-ray bursts where it was higher. The QPO was not detected in observation 1, when the count rate was a factor 2 to 3 higher than otherwise. The power spectral features show no changes that are correlated with variations of $\sim 20\%$ in the out-of-dip count rate, except for observations 8 to 10, in which the frequency is anti-correlated with the out-of-dip count rate. In addition to the QPO, a noise component at frequencies below 1 Hz was present, with a typical strength of 6%–10% rms. Both the QPO and the noise component have a flat photon energy spectrum.

Several of the properties of the QPO, notably its frequency, its relatively unchanged persistence during bursts and dips, and its flat energy spectrum, are remarkably similar to those of the ~ 1 Hz QPO that was recently found by JO99 in 4U 1323–62. Figure 2 shows that the ratio of frequency to FWHM of the QPO in 4U 1323–62 is also consistent with 3.5, and Figure 3 shows that the noise component in 4U 1323–62 falls on the strength versus slope relation found for the noise component in EXO 0748–676. We conclude that both QPOs are produced by the same mechanism. Since QPOs like these have not been seen in other neutron star LMXBs the origin is most likely related to the high inclination of the sources (JO99). It is unlikely that the QPOs are produced by variations in mass accretion rate (\dot{M}) onto the neutron star: in that case they should also be visible in low-inclination sources. Moreover, other QPOs that are thought to be

produced by \dot{M} variations, show considerable energy dependence (van der Klis 1995). A medium modulating the radiation from a central source (JO99) seems to be a more promising explanation (see below).

We have found several new features of the QPO, that were not seen in 4U 1323–62. First, the large flux range in the observations of EXO 0748–676 allow us to say that the QPO is not present at high persistent count rates. In 4U 1323–62, whose flux varied by only $\sim 15\%$, the QPO was always present. Second, the properties of the QPO changed during three of the four bursts. In 4U 1323–62 the properties of the QPO remained the same during all bursts. Third, there is the difference in frequency range over which the QPOs are observed: a factor ~ 4 in EXO 0748–676 and $\sim 12\%$ in 4U 1323–62. This could be due to the difference in the time span over which the sources were observed. 4U 1323–62 was observed for two consecutive days, whereas the EXO 0748–676 observations span 19 months. The $\sim 12\%$ range in two days, is similar to the $<15\%$ range found for individual observations (~ 1 day) of EXO 0748–676. Finally, the noise has a flat photon spectrum, which suggests that the mechanism behind the noise is similar to that for the QPO.

Much can be learned about the QPO from its behavior during the X-ray bursts. The fact that the QPO is detected during all four bursts shows that the presence of the QPO does not directly depend on the instantaneous flux, and that the absence of the QPO in observation 1 is due to something else than just a higher count rate. Since the fractional rms amplitudes during the bursts are similar to those outside the bursts, variations in \dot{M} onto to neutron star can be ruled out as the origin of the QPO. A dramatic decrease in rms amplitude is expected in that case. The high count rates during the X-ray bursts enables us to detect the QPO in smaller time intervals, typically tens of seconds, than otherwise possible. In all bursts the Q of the

QPOs is higher than 3.5, and during three of the bursts we see the frequency shift. This seems to indicate that the QPO is intrinsically narrower than measured by us. The observed width of the QPO outside the bursts is then due to changes of the QPO frequency on time scales of a few hundred seconds, and/or due to the presence of several QPOs with a higher Q that occur around a central frequency.

We now consider models that involve modulation of radiation from a central source. Given the inclination of EXO 0748-676 (75° – 82°), to be in the line of sight to the central source, a medium modulating the radiation from the central source must at least reach a height that is between 14% and 27% of its radial distance to the central source. De Jong, van Paradijs, & Augusteijn (1996) found that accretion discs in LMXBs have opening semi-angles of $\sim 12^\circ$ as seen from the central source. Hence only a small height above the accretion disc is required, typically a few percent of the radial distance to the neutron star, to be in the line of sight. This suggests that the modulating medium is in or on the disc. Any model is constrained by the fact that the rms amplitude stays constant when the source goes into a dip; the medium causing the dips has to remove more or less the same amount of modulated as unmodulated radiation from our line of sight. Models can be constructed, with varying geometries that depend on whether the central source is point-like or extended, and whether the media causing the dips and QPO are absorbing or scattering media. Only a few combinations can be ruled out with certainty, e.g. most models involving a point-like source. If the dips are being caused by a partial covering opaque medium, the central source has to be extended, and the medium causing the QPO should have an azimuthal extent comparable to that of the medium causing the dips, in order to explain the constancy of the rms amplitudes in- and outside the dips. The mechanism also has to produce a central frequency that does not vary by more than 15% over the dura-

tion of a single observation (typically one day).

Both partial covering by an opaque medium (see JO99) and Thomson scattering can explain the flat photon spectrum of the QPO. Assuming the QPO frequency is the Kepler frequency of a structure orbiting a $1.4 M_\odot$ neutron star, one derives radial distances of 1.0 – 2.4×10^8 cm. The viscous timescale (Frank, King, & Raine 1992) at these radii, on which the orbiting structure is expected to alter, is comparable to the timescales that are seen for the frequency shifts during the burst. The larger frequency changes between observations might be related to the timescale on which the accretion disc as a whole changes its structure (typically days to weeks). We remark that the inferred radii are similar to those in the α -disc model (Frank et al. 1992), at which the dominant opacity source changes from Kramers' opacity to electron scattering. This radius increases with \dot{M} , and implies an anti-correlation between frequency and count rate, as seen in observation 8–10.

The fact that the QPO is not found in observation 1 suggests that the higher count rate is accompanied by a change in the accretion disc structure. Both are probably due to an increase in \dot{M} . Assuming that an accretion disc thickens with \dot{M} , the modulated flux might be obscured by a thicker disc, but the mechanism may also have disappeared altogether.

Finally we remark that the 0.15 s jitter in the mid-eclipse timings reported by Hertz et al. (1997) might be due the presence of the QPO reported here. A QPO with a frequency of 1 Hz and an rms amplitude of 10%, arbitrarily superimposed on eclipse transitions lasting a few seconds, can be expected to cause a jitter in the order of 0.1 s.

This work was supported in part by the Netherlands Foundation for Research in Astronomy (ASTRON). JVP acknowledges NASA support. This research has made use of data obtained through the HEASARC Online Service, provided

by the NASA/GSFC.

REFERENCES

- Bradt, H.V., Rothschild, R.E., Swank, J.H., 1993, A&AS, 97, 355
- Church, M.J., Bałucińska-Church, M., Dotani, T., Asai, K., 1998, ApJ, 504, 516
- de Jong, J.A., van Paradijs, J., Augusteijn, T., 1996, A&A, 314, 484
- Frank, J., King, A.R., Lasota, J.-P., 1987, A&A, 178, 137
- Frank, J., King, A., Raine, D., 1992, Accretion Power in Astrophysics (Cambridge; Cambridge Univ. Press)
- Hertz, P., Wood, K.S., Cominsky, L.R., 1997, ApJ, 486, 1000
- Jahoda, K., Swank, J.H., Giles, A.B., Stark, M.J., Strohmayer, T., Zhang, W., Morgan, E.H., 1996, SPIE, 2808, 59
- Jonker, P.G., Van der Klis, M., & Wijnands, R., 1999, ApJ, in press (astro-ph/9811404)
- Parmar, A.N., White, N.E., Giommi, P., & Haberl, F., 1985, IAU Circ., 4039
- Parmar, A.N., White, N.E., Giommi, P., & Gottwald, M., 1986, ApJ, 308, 199
- van der Klis, M., 1995, in X-ray Binaries, ed. W.H.G. Lewin, J. van Paradijs, E.P.J. van den Heuvel (Cambridge: Cambridge Univ. Press)
- Walter, F.M., Bowyer, S., Mason, K.O., Clarke, J.T., Henry, J.P., Halpern, J., Grindlay, J.E., 1982, ApJ, 253, L67
- White, N.E., Swank, J.H., 1982, ApJ, 253, L61

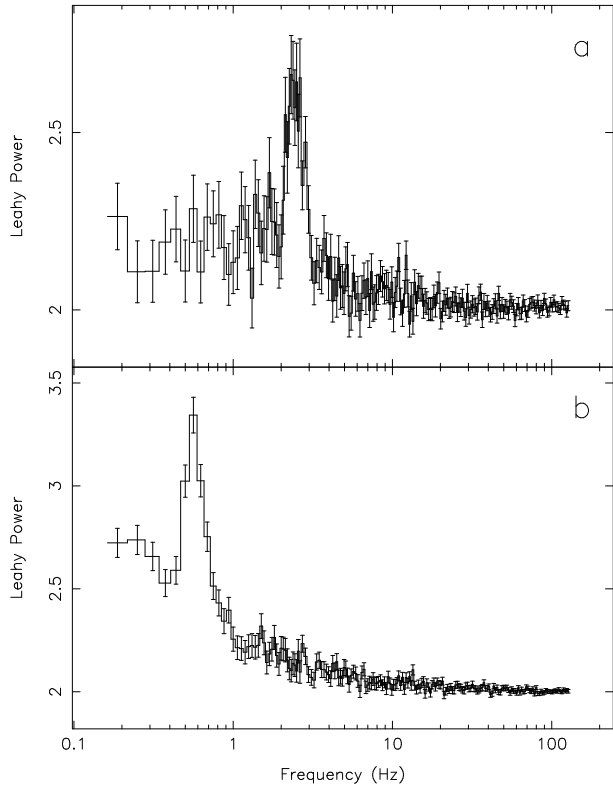


Fig. 1.— The power spectra of observations 2 (a) and 10 (b), showing the QPO at 2.44 ± 0.03 Hz and at 0.58 ± 0.01 Hz, respectively.

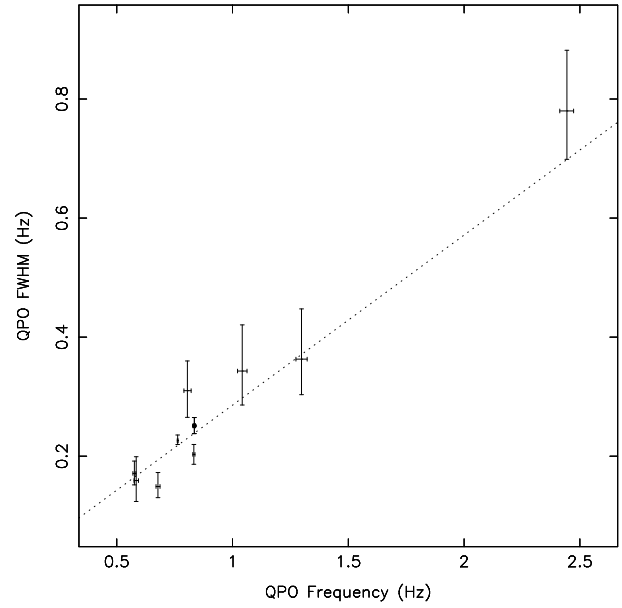


Fig. 2.— The QPO FWHM as a function of the QPO frequency. The dotted line is the best fit for a constant Q ($Q=3.5$). The black dot represents the value obtained for 4U 1323–62 (JO99).

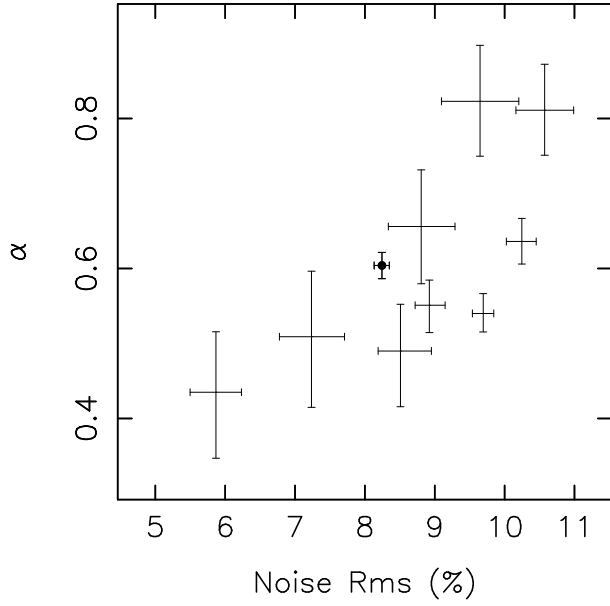


Fig. 3.— The power law index, α , of the noise component as a function of the noise rms amplitude. The black dot represents the value obtained for 4U 1323–62.

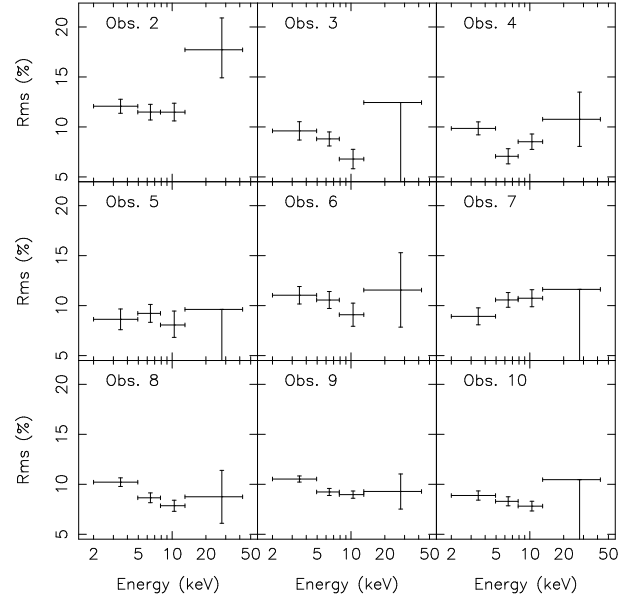


Fig. 4.— The energy dependence of the QPO strength (dip and non-dip data combined). The points without positive rms errors are upper limits.

TABLE 1

LOG OF THE *RXTE* OBSERVATIONS OF EXO 0748–676, AND THE POWER SPECTRAL FIT PARAMETERS FOR EACH OF THEM. THE FIT PARAMETERS ARE FOR ALL DATA (DIP AND NON-DIP) COMBINED. FOR EACH BURST THE QPO PARAMETERS ARE GIVEN BELOW THE OBSERVATION IN WHICH THEY OCCURRED; FOR BURST 4 THE FIT PARAMETERS OF BOTH LORENTZIANS ARE GIVEN.

Obs. ^a	Begin (UTC)	End (UTC)	T_{OBS}^b (ks)	QPO			Noise		Count rate ^c (counts s ⁻¹)	
				rms (%)	FWHM (Hz)	Frequency (Hz)	rms ^d (%)	PLI		
1	12-03-96 10:41	12-03-96 12:54	6.0 (0.9)	< 2.1 ^e	—	—	3.8±0.2	0.98±0.12	177.2±0.3	
2	03-05-96 08:37	04-05-96 00:30	12.0 (2.9)	12.1 ^{+0.6} _{-0.6}	0.8±0.1	2.44±0.03	5.7±0.4	0.43±0.09	72.9±0.3	
3	18-01-97 17:14	19-01-97 13:18	9.6 (3.7)	8.8±0.7	0.16±0.04	0.58±0.01	9.6±0.6	0.82±0.07	62.7±0.2	
4	07-03-97 20:03	08-03-97 12:40	9.8 (5.6)	8.9±0.5	0.15±0.02	0.68±0.01	10.6±0.4	0.81±0.06	59.6±0.2	
5	01-05-97 11:52	02-05-97 07:25	9.5 (3.3)	9.3 ^{+0.8} _{-0.6}	0.36±0.07	1.30±0.02	7.2±0.5	0.51±0.09	64.9±0.3	
				Burst 1	9.7±0.9	0.18±0.5				1.41±0.02
6	26-06-97 06:01	26-06-97 22:03	9.7 (2.7)	9.8 ^{+0.8} _{-0.6}	0.34±0.07	1.04±0.02	8.8±0.5	0.67±0.08	60.9±0.2	
7	07-10-97 00:51	07-10-97 20:32	8.6	9.9±0.6	0.31±0.05	0.81±0.02	8.5 ^{+0.4} _{-0.3}	0.49±0.07	68.3±0.3	
8	13-08-97 19:38	14-08-97 03:02	17.3 (1.7)	9.1±0.3	0.20±0.02	0.833±0.005	8.9±0.2	0.55±0.04	69.0±0.1	
				Burst 2	8.4±1.1	0.2±0.1				0.84±0.02
9	17-08-97 12:41	17-08-97 18:59	36.7 (6.9)	10.4±0.2	0.23±0.01	0.763±0.002	9.7±0.2	0.54±0.03	72.5±0.1	
				Burst 3	7.1±0.9	0.11±0.03				0.75±0.02
				Burst 4	7.3±1.3	0.11±0.07				0.89±0.02
10	22-08-97 00:13	22-08-97 18:56	24.5 (10.1)	6.7 ^{+2.8} _{-1.6}	0.13 ^{+0.17} _{-0.06}	0.65 ^{+0.03} _{-0.05}	10.2±0.2	0.64±0.03	75.3±0.2	
				Burst 4	8.4±0.4	0.17±0.02				0.58±0.01

^aObs. IDs are 10068–03–01–00, 10108–01–(01–05), 20069–(02–06), and 20082–01–(01–03) for respectively obs. 1, 2, 3 to 7, and 8 to 10.

^bTime in dips (see section 2) is given between brackets. For observation 7 this could not be determined accurately.

^cThe average 2–60 keV count rate (3 detectors; dips, eclipses and bursts excluded), obtained from the Standard 2 data.

^dThe noise rms is integrated from 0.1 to 1.0 Hz.

^eFor the frequency range 1–10 Hz and for an assumed Q of 3.5